Photodissociation of acetone at 193 nm: Rotational and vibrationalstate distributions of methyl fragments by diode laser absorption/gain spectroscopy

G. E. Hall, D. Vanden Bout, and Trevor J. Sears

Citation: The Journal of Chemical Physics **94**, 4182 (1991); doi: 10.1063/1.460741
View online: http://dx.doi.org/10.1063/1.460741
View Table of Contents: http://scitation.aip.org/content/aip/journal/jcp/94/6?ver=pdfcov
Published by the AIP Publishing

Photodissociation of acetone at 193 nm: Rotational- and vibrational-state distributions of methyl fragments by diode laser absorption/gain spectroscopy

G. E. Hall, D. Vanden Bout,[a] and Trevor J. Sears
Department of Chemistry, Brookhaven National Laboratory, Upton, New York 11973

(Received 23 October 1990; accepted 12 December 1990)

Diode laser transient absorption/gain spectroscopy is used to monitor time-dependent populations of CD_3 fragments formed in the photodissociation of acetone-d_6 at 193 nm. Selected rotational lines have been measured in the ν_2 "umbrella" fundamental and first two hot bands, and in the ν_3 asymmetric stretching fundamental band. Substantial growth is observed in the vibrationless state on the time scale of vibrational relaxation. We estimate that only about 15% of the nascent CD_3 population is formed in the vibrational states we detect: $\nu_2 = 1$ and 2, $\nu_3 = 1$, and the vibrationless state. Most of the nascent methyl population is evidently spread among many undetected vibrational states. These results complement previous measurements of acetone photofragments by infrared emission, multiphoton ionization, and laser-induced fluorescence. Our inferred global vibrational distribution is consistent with a two-step fragmentation.

I. INTRODUCTION

Three fragments emerge from the deep ultraviolet photodissociation of acetone. The application of state-resolved detection to the polyatomic fragments of such a process poses new challenges to our understanding of small molecule photodissociation reactions. The two chemically identical methyl radicals hold in their nascent energy distribution a clue to their origins. One might hope to distinguish between a mechanism that produces CO and both methyl radicals simultaneously and a mechanism that involves a transient CH_3CO radical by interpreting the fragment energy, momentum, and angular momentum distributions. We report diode laser absorption/gain measurements of vibration–rotation populations in the vibrationless state and the excited ν_2 and ν_3 modes of CD_3. The nascent populations in all the detected levels are small compared to the growth in the vibrationless level that occurs on the time scale of vibrational relaxation. Most nascent CD_3 radicals thus appear to be in other, undetected vibrational levels.

The photophysics and photochemistry of acetone excited to its lowest $^1(n,\pi^*)$ excited state at wavelengths longer than 200 nm have been extensively studied and reviewed.[1-5] The primary photoproducts of acetone in this special region are $CH_3 + CH_3CO$, with a strong dependence on pressure, temperature, and excitation wavelength. At low pressures, dissociation primarily occurs from vibrationally excited levels of the strongly mixed $^1(n,\pi^*)$ and $^3(n,\pi^*)$ states. At higher pressures, there is a temperature dependent dissociation of both the vibrationally relaxed triplet and the acetyl radical to yield a second methyl radical and CO.

A stronger absorption to the S_2 state of acetone, a $^1(n,3s)$ Rydberg state, begins at about 200 nm. Product analysis by Potzinger and Von Bünau following 185 nm photolysis found CO and C_2H_6 in amounts consistent with $CO + 2CH_3$ as the primary step.[6] Recent time-resolved absorption measurements and product analysis by Pilling and co-workers[7-8] have found the quantum yield for $CO + 2CH_3$ to be 0.95 at 193 nm. Minor product channels identified include $H + CH_2COCH_3$ and $CH_4 + CH_2CO$. From the intensity dependence of the CH_3CO^+ and $CH_3COCH_3^+$ yield in focused 193 nm light, Baba *et al.*[9] inferred the existence of neutral CH_3CO as a transient intermediate in the one-photon dissociation. The absorption spectra of acetone and acetone clusters in a supersonic jet have been measured by Vaida and co-workers.[10,11] From changes in the vibronic structure with clustering, they have inferred a predissociative mechanism for the decomposition of the S_2 state.

Product state distributions have been reported for CO and CH_3 photofragments following excitation at 193 nm. The CO energy distribution has been studied by infrared emission[5,12] and laser-induced fluorescence.[13] Extensive rotational excitation is observed, inconsistent with a planar, symmetric dissociation, although a symmetric minimum energy exit channel does not guarantee uniformly symmetric dissociations.[13] Infrared emission from CH_3 at 2700–3500 cm^{-1} has been detected with low resolution (30–60 cm^{-1}) and assigned to sequence bands (1–0), (2–1), and (3–2) of the infrared active CH stretching mode ν_3.[12] Nascent methyl fragments have also been detected by resonance enhanced multiphoton ionization (REMPI) in a time-of-flight mass spectrometer that also provides kinetic energy and angular resolution.[13]

The present work complements previous state-resolved measurements by providing complete rotational resolution to the methyl detection, using a technique that gives easily calibrated relative populations, unlike REMPI. The diode laser absorption/gain technique can be used to monitor the vibrationless state, unlike ir emission. By following the transient absorption signals during vibrational relaxation, we can estimate the fraction of nascent methyl photofragments in the internal energy states we probe.

[a] Present address: Department of Chemistry, University of Texas at Austin, Austin, Texas 78712.

 0021-9606/91/064182-07$03.00

Deuterated acetone has been used in this study primarily because the diode lasers we have operate in the spectral region appropriate for monitoring CD_3 and not CH_3. The dissociation dynamics of acetone-h_6 and acetone-d_6 may differ, suggesting caution in comparing our results to those for acetone-h_6. We note, however, that the dramatic differences between the $^1(n\text{-}\pi^*)$ photoprocesses of H_2CO and D_2CO are reduced to only minor differences between acetone-h_6 and acetone-d_6.[2,14]

II. EXPERIMENTAL

The apparatus for time-resolved diode laser absorption/gain measurements has been described in previous publications.[15,16] The essential components are a 2 m glass flow cell through which neat acetone-d_6 vapor (Aldrich, 99 + atom D) is slowly pumped at a pressure of 4 Pa (1 Pa = 7.5×10^{-3} Torr). The acetone is dissociated at 193 nm by an excimer laser (Questek model 2240) using 15 mJ/pulse in a 7 mm diameter beam at 4 Hz. The quartz entrance window gradually accumulates a sooty deposit where the excimer laser enters the sample cell, so the actual 193 nm intensity in the flow cell can be less. The tunable diode laser beam (Laser Photonics, Analytics Div.) is collimated and launched into the 2 m flow cell, making eight round trips between White cell mirrors before leaving the flow cell. Approximately 60% of the 32 m diode laser optical path is overlapped with the nearly collinear excimer laser beam, based on the signal enhancement compared to a single pass, collinear probe geometry. After leaving the sample cell, the diode laser beam passes through a monochromator for mode selection and onto a liquid He-cooled Cu:Ge detector for the ν_2 bands at 450–700 cm^{-1}, or a liquid N_2-cooled InSb detector for the ν_3 band near 2300 cm^{-1}. With the load resistors and preamplifiers used, the response time was 1–2 μs for each detector, corresponding to about 0.5 gas kinetic collisions at 4 Pa. A transient recorder (LeCroy 8828C) interfaced to an 80286 lab computer collected time-dependent signals at a fixed infrared frequency; a boxcar system was used for scanning frequency at a fixed delay. For each transient measurement at fixed frequency, the transmitted diode laser intensity prior to photolysis I_0 was determined using a chopper wheel and an oscilloscope. The ac-coupled transient absorption intensities were combined with I_0 to calculate a time-dependent absorbance. Background signals, consisting of electrical noise synchronous with the excimer laser and a delayed acoustic oscillation, were measured for subsequent subtraction with the diode laser tuned off resonance. This background subtraction was found to be insignificant for all but the three weakest signals used in the data analysis, for which the maximum absorbance was less than 0.01.

Under the flow conditions, photolysis energies and repetition rates used, the illuminated sample pressure was elevated by about 10%–15% compared to the steady-state pressure in the dark. We presume the photolytic accumulation of CO + C_2D_6 is responsible for this pressure rise. Higher repetition rates or slower pumping of the deuterated sample increased the pressure rise further, but did not have a significant effect on the transient signals.

III. RESULTS

A. Populations in the ν_2 mode

The high-resolution spectrum of CD_3 in the ν_2 fundamental region has more than a thousand lines. The amplitude of each line probes the time-dependent difference in population of a pair of rotational states with different vibrational energies. At thermal equilibrium, the upper and lower state populations are related by a Boltzmann factor, and the spectral intensities contain highly redundant information: the entire spectrum can be characterized by a single temperature. The internal energy distributions of nascent photofragments need not, and generally cannot, be described by a temperature. The principal problem of experimental design is to avoid an unmanageably large set of measurements, while making only testable assumptions in the data analysis. We have chosen to measure time-dependent absorption/gain signals for a small subset of rotational lines, spanning rotational energies from 0 to 1500 cm^{-1}, attempting to record the same rotational Q branch lines in each vibrational band. This choice of lines simplifies the determination of relative populations from a set of measured population differences, as described below.

The rotational lines used in the population analysis are listed in Table I. We have limited our measurements to the strong $K = N$ and $K = N - 1$ subbands, as the Q branch line strength factors are $K^2/N(N+1)$. Assignments are from the earlier work of Sears *et al.*[17] Some of the lines were not recorded in the earlier spectroscopic work, but predictions using the published constants were found to be very reliable. For each rotational transition, acceptable signals were obtained by averaging the transients from 25 laser shots. Multiple measurements typically resulted in indistinguishable transient signals, apart from an overall amplitude variation of $\pm$ 10%. Two to four separate measurements were averaged for each rotational transition. A few lines in the (4–3) band could also be detected, but the time-dependent signals were too weak to be measured accurately.

Measured absorbance was converted to population differences using Eq. (1):

$$-\log\left[\frac{I_0 - I_{\rm abs}(\nu_0)}{I_0}\right] \propto (n_i - n_j) S_{ji} \nu_0 |\mu_v|^2 g(\nu_0), \qquad (1)$$

where I_0 and $I_{\rm abs}(\nu_0)$ are the incident and absorbed diode laser intensities at ν_0, the transition frequency, n_i and n_j are the number densities of the lower and upper vibration–rotation state, S_{ji} is the rotational line strength, $K^2/N(N+1)$

TABLE I. Rotational lines used in CD_3 ν_2 population analysis.

(1–0) band		(2–1) band		(3–2) band	
Line	cm^{-1}	Line	cm^{-1}	Line	cm^{-1}
$Q(3,2)$	457.183	$Q(3,2)$	507.236	$Q(3,2)$	541.5693
$Q(11,11)$	460.017	$Q(11,11)$	509.610	$Q(11,10)$	541.192
$Q(13,13)$	461.099	$Q(13,12)$	507.471		
$Q(16,15)$	459.343			$Q(15,15)$	545.525
$Q(19,18)$	461.024	$Q(19,18)$	509.646	$Q(18,18)$	547.298
$Q(21,21)$	467.414	$Q(21,21)$	515.797	$Q(6,5)$	541.115
$Q(24,24)$	470.570			$Q(5,4)$	541.225

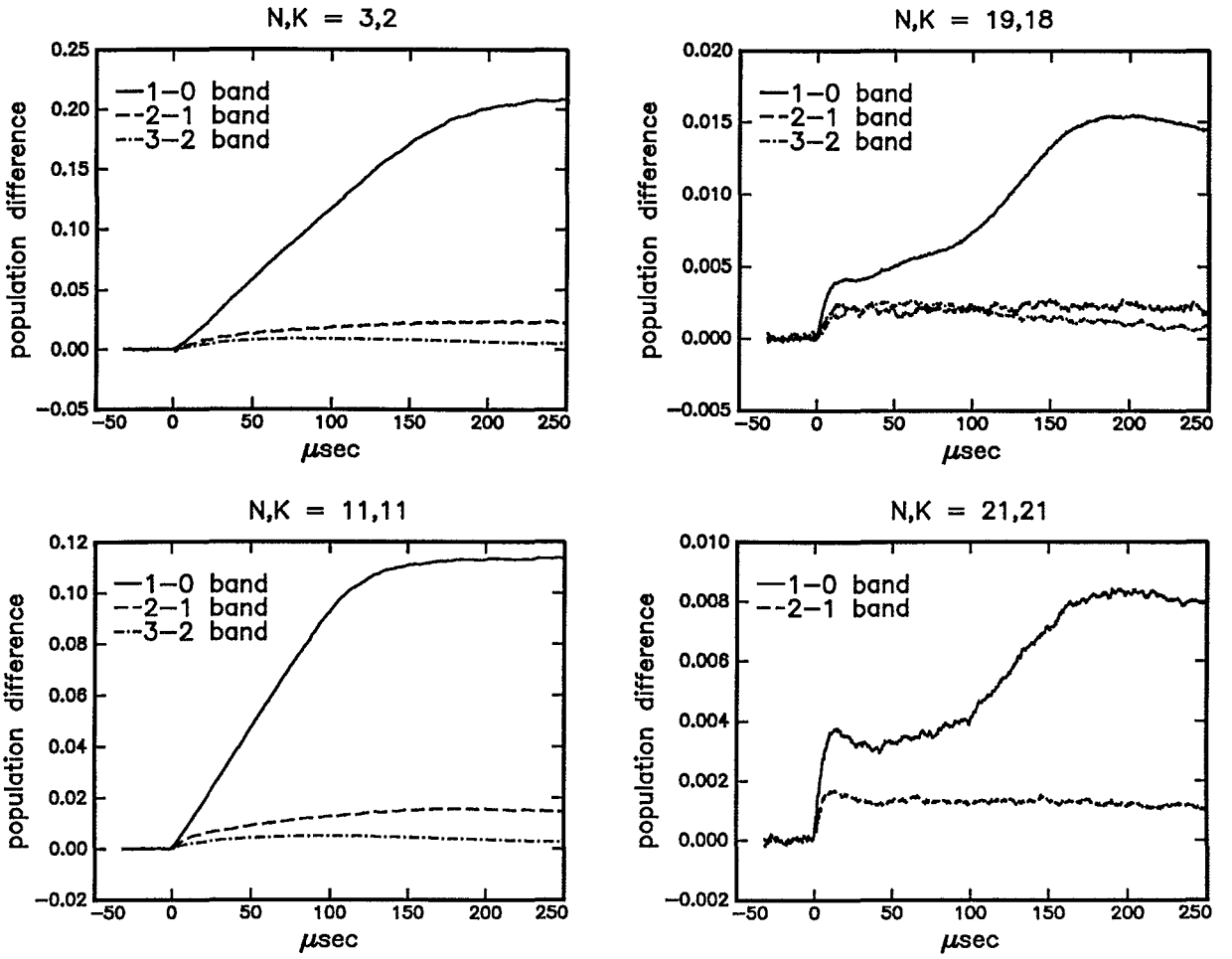

FIG. 1. Time-dependent population differences for four rotational levels, derived from three vibrational bands. Each line is a raw absorbance signal, corrected for rotational line strength, vibrational transition moment, transition frequency, and photolysis laser energy according to Eq. (1). The relative magnitudes of the population differences are directly comparable following this scaling.

for Q branch transitions, $|\mu_v|^2$ is the vibration-dependent transition moment,[15] and $g(\nu_0)$ is the maximum value of a normalized Doppler line shape function. Figure 1 illustrates time-dependent population differences for four rotational levels in the first three vibrational levels of the ν_2 mode. In each case, the population differences are positive (no gain is observed), and the population differences decrease at higher vibrational levels. The advantage of measuring Q branch intensities for the same rotational lines in different vibrational bands becomes clear when estimating relative populations from a set of population difference measurements. A complete sum of population differences gives the population of the lowest level:

$$n_{0,N,K} = (n_{0,N,K} - n_{1,N,K}) + (n_{1,N,K} - n_{2,N,K}) + (n_{2,N,K} - n_{3,N,K}) + \cdots . \quad (2)$$

Each term in parentheses can be determined from a Q branch absorption intensity, and when the sum is truncated after i terms, the truncation error is exactly $-n_{i,N,K}$. While we cannot assign confidence limits to unmeasured quantities, the observed decrease in population differences at higher vibrations makes the neglect of $n_{3,N,K}$ compared to $n_{0,N,K}$ seem a good approximation. If the population of $v = 3$ is described by the same vibrational temperature we deduce below for the three lower ν_2 states, the truncation error would be 1%–5% at late and early times, smaller than the measurement errors. Time-dependent populations of the $v = 0$ rotational levels probed by (1–0) band transitions were estimated with Eq. (2), truncated after the three terms written. Similarly, $v = 1$ populations were estimated with a sum of (2–1) and (3–2) band measurements, and $v = 2$ populations were approximated directly from the measured $n_{2,N,K} - n_{3,N,K}$ population differences. The truncation errors will be progressively worse for $v = 0,1$, and 2. For the cases where identical N,K lines were not measured in each band, a measured line for a nearby rotational state was corrected by a scaling factor close to one, obtained from a Boltzmann fit to the peak absorption amplitudes.

While the rotational distributions arising from photodissociation generally need not be described by a temperature, we find the rotational populations sampled at a fixed time can be well represented by thermal distributions:

$$n_{v,N,K} = n_v g_{N,K} \frac{\exp(-E_{\rm rot}/kT)}{Q_{\rm rot}}, \quad (3)$$

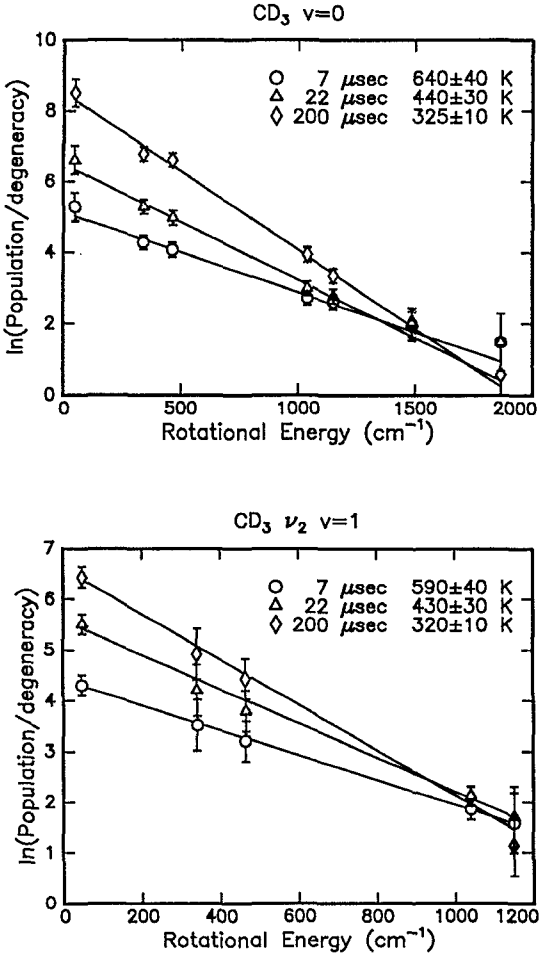

FIG. 2. Rotational Boltzmann plots at three times for $v = 0$ and $v_2 = 1$.

where n_v is the sum of rotational population in the vth vibrational state, E_{rot} is the rotational energy of the level with quantum numbers N and K, Q_{rot} is the (temperature dependent) rotational partition function, and $g_{N,K}$ is the degeneracy weight of the level. A plot of $\ln(n_{v,N,K}/g_{N,K})$ vs E_{rot} at a fixed time gives a line with a slope of $-1/kT$ and an intercept of $\ln(n_v/Q_{rot})$. The results of several of these plots are shown in Fig. 2 for $v_2 = 0$ and $v_2 = 1$. The rotational temperatures for each vibrational state studied is initially about 700 K and converges to 320 ± 10 K at times $> 100\ \mu$s, as illustrated in Fig. 3. Extrapolations of the time-dependent rotational temperatures to zero time lead to nascent T_{rot} of 750 ± 100, 620 ± 100, and 600 ± 100 K in $v_2 = 0,1$, and 2.

The intercepts of plots like those of Fig. 2 give a time-dependent value for $\ln(n_v/Q_{rot})$ that, together with the calculated, temperature-dependent partition function, allow us to estimate n_v at 5 μs increments for $v = 0$, 1, and 2, illustrated in Fig. 4. The nonlinear rise at the earliest times we identify with the effects of translational moderation, which causes a depression of the early absorption signals measured by a narrow band laser before the nascent Doppler-broadened line shape collapses to its final, room-temperature value. The factor $g(\nu_0)$ in Eq. (1) increases as the translational temperature drops. We attempted to record the Doppler-broadened line shapes at short delay times, but the signals were too

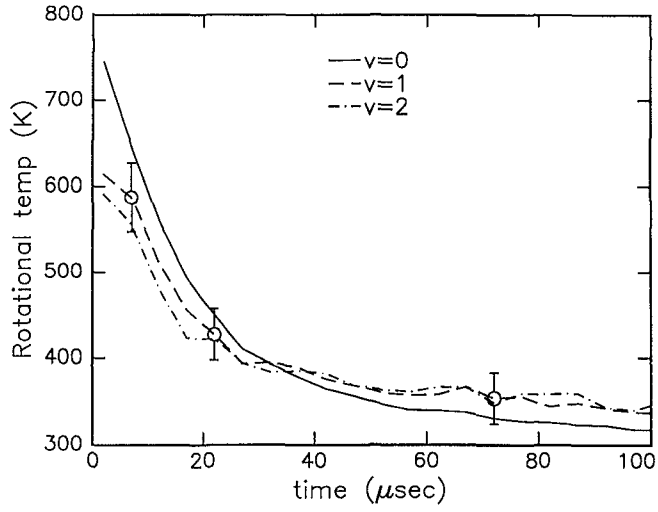

FIG. 3. Time-dependent rotational temperatures for $v_2 = 0$, 1, 2.

small to make these measurements reliably. Based on previous measurements in this apparatus,[15] we expect the Doppler relaxation to have a characteristic time of 10–15 μs at this pressure.

From Fig. 4 we see that while the populations in $v_2 = 1$ and $v_2 = 2$ are small and slowly changing from approximately 30 out to 250 μs following the dissociation event, the $v = 0$ population grows substantially during the first 180 μs. The nearly linear growth in $v = 0$ encourages us to use a linear extrapolation back from times later than 20 μs to correct for the effect of changing $g(\nu_0)$ at early times. This extrapolated nascent total population in $v = 0$ as a fraction of the maximum CD_3 population is only 0.06 ± 0.03. The populations in $v = 1$ and 2 of the ν_2 mode are smaller by successive factors of about three, well described by an initial vibrational temperature of 750 K for these three points.

B. Population in the ν_3 mode

Excitation in the CH_3 ν_3 mode has been observed by Donaldson and Leone,[12,18] following 193 nm photolysis of

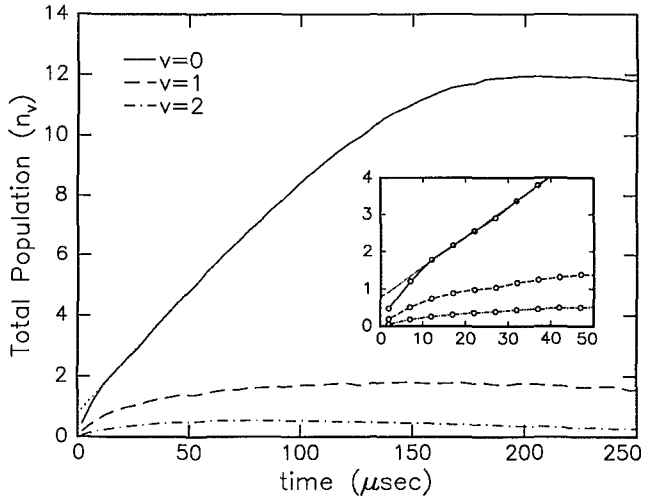

FIG. 4. Rotationally summed populations for $v_2 = 0,1,2$. The inset shows an expanded view of the first 50 μs, and the dotted extrapolation to $t = 0$ that corrects for Doppler linewidth relaxation.

acetone. Vibrational relaxation of the ν_3 mode of CH_3 by acetone has a reported rate constant of $8.1 \pm 0.9 \times 10^{-12}$ cm^3 s^{-1}.[18] The large rate constant for acetone compared to inert gases was attributed to a near-resonant V–V process, which should produce vibrationally cold CH_3, while other collision partners act to redistribute the CH_3 vibrational energy into lower frequency modes. At 4 Pa and 300 K, this corresponds to a 130 μs lifetime for the acetone quenching of ν_3 emission, in reasonable agreement with our observed growth rate of $v = 0$. If $v_3 = 1$ is the primary source of the growth of $v = 0$, there should be immense gain on the ν_3 (1–0) band. The ν_3 fundamental of CD_3 has recently been detected and assigned at high resolution,[19] permitting us to measure time-dependent absorption signals on several rotational transitions. All showed only positive absorption at short times; a typical example is illustrated in Fig. 5 for the $^rR(7,6)$ transition at 2410.4964 cm^{-1}. The time-dependent signals were generally very similar to the analogous rotational lines of the ν_2 (1–0) band, apart from a 10-20 times weaker signal, under comparable experimental conditions, due to the weaker transition moment. Since we have not measured or assigned transitions involving higher v_3 quantum numbers, it was not possible to perform the same detailed analysis of the ν_3 populations as we have for ν_2. However, the absence of gain for all rotational states detected confirms that $n_{v=1} < n_{v=0}$ for ν_3. An upper limit on the total nascent population accounted for in $v = 1$ and 2 of ν_2, $v = 1$ of ν_3, and the vibrationless state is thus only about 15%.

C. Diffusion and radical recombination

The effects of diffusion and methyl recombination were investigated by pressure dependent studies on low rotational lines of the 1–0 ν_2 band. These lines have a time dependence qualitatively similar to the total population of the vibrationless state, as seen in Figs. 1 and 4. Adding several hundred Pa of Ar or He to the acetone sample increased both the growth and decay rate without making large changes in the maximum amplitude compared to neat acetone-d_6. The faster growth is consistent with accelerated vibrational relaxation, and for the faster decay is consistent with accelerated methyl recombination in the falloff region.[20] If the effects of diffusion were significant in the low pressure, neat acetone measurements, adding buffer should increase the peak signals. This did not occur. The probed volume is larger than the photolysis volume in our multipass geometry[16] and despite the low pressure, the transient absorption kinetics do not seem significantly perturbed by diffusion at times less than 200 μs. Variation of the pressure of neat acetone produced linear changes in the growth rates and the peak absorption amplitudes.

IV. DISCUSSION

A. Comparison with other work

The nascent rotational and ν_2 vibrational temperatures that we measure are consistent with the CH_3 REMPI results[13] of $\sim$500 and $\sim$800 K. However, our results suggest that these ν_2 levels studied represent only about 10% of the nascent CD_3 formed in the dissociation. Where is the growing population of cold methyl radicals coming from? The lifetime of any excited state precursor to dissociation is clearly not in the 100 μs regime, and the secondary photochemistry[7,8] has no delayed formation of methyl radicals. Unmeasured rotational lines, either for low K or higher N levels could conceivably account for missing nascent population, although the $v = 0$ population continues to grow even after rotational thermalization. The reasonable agreement of our extrapolated rotational and vibrational distributions with the collisionless REMPI measurements[13] supports our use of the Boltzmann analysis to obtain rotationally summed nascent populations, and argues against serious errors in our measurements due to collisions that transfer methyl kinetic energy into internal energy.

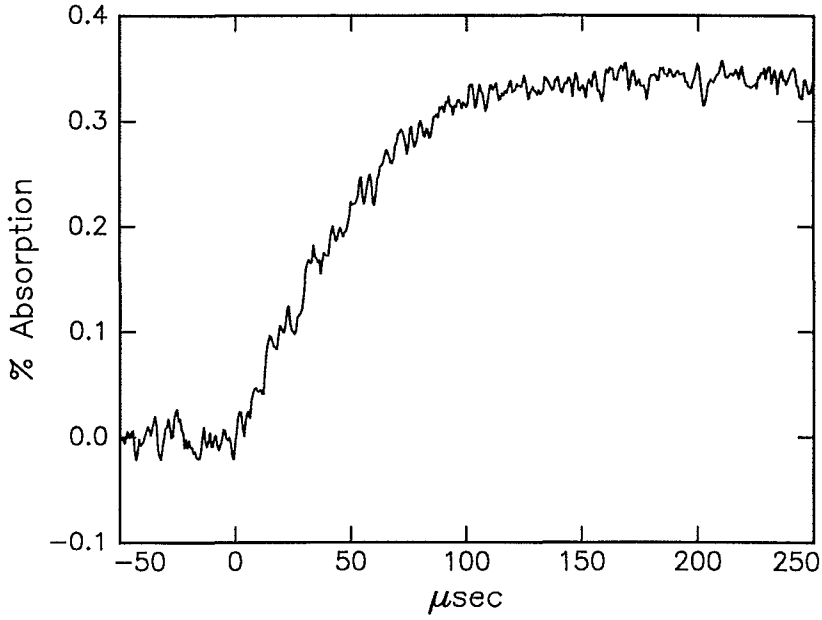

FIG. 5. Absorption signal for a typical ν_3 1–0 band transition: $^rR(7,6)$ transition at 2410.4964 cm^{-1}. The time dependence is similar to that observed for the ν_2 fundamental for similar rotational levels.

The spectra of CD_3 we measured in the 450–520 cm^{-1} region contain many weaker absorption lines that we have tentatively assigned to $\nu_2 + \nu_4 \leftarrow \nu_4$ or other $\Delta v_2 = 1$ transitions in combination states. These lines show transient absorption kinetics with faster, although not detector limited, rise times and decay within 300 μs. All of the observations are explained if the CD_3 radicals formed on dissociation of acetone are produced in a large number of vibrational states with no strong preferences for any particular vibrational mode. The available energy for the three fragments following 193 nm dissociation is 221 kJ/mol. Equipartition of the available energy among all degrees of freedom of $CO + 2CD_3$ would provide about 5500 cm^{-1} of total vibrational energy in each CD_3; there are more than 150 vibrational states below this energy in CD_3. If the population is truly spread out over all these states, this requires that the nascent infrared emission spectrum of the radical consist of many weak lines derived from combination states leading to a very dense spectrum in the ν_2 fundamental region. Also the nascent ν_3 emission will not be composed simply of 1–0, 2–1, 3–2, and higher bands as suggested previously[12] but may have contributions from many combination bands particularly involving excitation in the lower frequency (ν_2 and ν_4) modes. Tests of these predictions should be possible using the time-resolved FTIR emission technique,[5,21] particularly in the ν_2 region.

B. Fragment energy distributions and the dissociation mechanism

A major motivation for starting this work was to take advantage of the full rotational state resolution of diode laser absorption/gain spectra to shed light on the dissociation process following 193 nm excitation of acetone. The high rotational excitation observed for CO has been taken as evidence for a two-step process,[5,12] in which the first methyl radical is ejected in a direct process, followed by a unimolecular acetyl decomposition that could generate more rotational excitation than a symmetric, three body dissociation. In this case, we might expect to see a composite internal energy distribution for the methyl radicals; the first one with high translational energy and low internal excitation, and the second one with a broader distribution of internal energy states. Our measurements show no sign of this composite energy distribution. If the first methyl radicals had an internal energy distribution similar to methyl from other direct dissociations, such as from methyl iodide,[15] most of them would be in the states we observe, contrary to our observed low yield of $v_2 = 0,1$, and 2. *Both* methyl radicals apparently have significantly more vibrational excitation.

A new information theoretic approach to three-particle dissociations has been developed recently by Strauss and Houston[22,23] and applied to acetone, among other molecules. In this approach, a joint probability distribution for the vibration, rotation, and translation of each particle can be found that agrees with whatever experimental state distributions have been measured, and simultaneously maximizes the entropy of the joint distribution. The resulting joint distribution can then be used to predict other properties of the dissociation. In particular, each coincident triplet of kinetic energies determines the mutual angles among the fragment recoil directions, subject to linear momentum conservation. The maximum entropy joint distribution can be analyzed to give the distribution of kinetic energy triplets and hence the distribution of the angle between the coincident methyl recoil velocities. The distribution of this angle differs for a concerted three-body fragmentation and for a two-step dissociation when the second step is slower than the rotation of the energized intermediate. Using the CO and CH_3 fragment energy distributions from Trentelman *et al.*[13] the analysis of Strauss and Houston finds the two methyl radicals to have a bias toward parallel recoil, but with a broad enough distribution to put acetone in a case intermediate between the concerted and stepwise limits.[23]

Since it appears that the methyl data used in their analysis represents only a small fraction of the total methyl radicals, we have investigated the sensitivity of these calculations to the choice of methyl input data. The CH_3 vibrational distribution used in Strauss and Houston's analysis ascribed 76% of the methyl population to $v = 0$,[13] compared to 14% for a prior distribution[23] and our estimate, which is also low. As one limiting case, we repeated the analysis of Strauss and Houston[23] using *only* the distribution of total CO energy determined from the CO measurements from acetone-h_6[13] to constrain the three-particle joint probability distribution.[24] The predicted mild preference for the two methyl radicals to recoil in the same direction is virtually unchanged with this change in the input data. The translational energy of the CO fragment is the crucial information for predicting the angle between the methyl velocities, since the final CO velocity is a vector sum of recoils along two directions. In a further test, we find that by avoiding a simplifying approximation in the earlier calculations and treating the kinetic and internal energy of CO separately in the optimization procedure, the predicted correlation between the coincident methyl velocities vanishes. Our most correct treatment of the available data now is consistent with a fully stepwise mechanism, in which the acetyl intermediate lifetime is long enough to rotationally average the secondary fragmentation. Further details of this multidimensional surprisal analysis will be presented elsewhere.[25]

The density of vibrational states is substantially higher for CD_3 than for CH_3, and this affects the prior distributions. For the dissociation of acetone-d_6 at the same dissociation energy, the three-particle prior distribution includes only 5% vibrationless CD_3 radicals. When we repeat the maximum entropy calculation for acetone-d_6, using the CO data measured from acetone-h_6 (perhaps a seriously poor approximation), the fraction of vibrationless CD_3 radicals is 10%. Our analysis of diode laser data gave an estimate of 0.06 ± 0.03 for this fraction in $v = 0$. This small fraction in $v = 0$ is close to the least surprising result, given the measured CO distribution, suggesting that most vibrational modes of both methyl radicals are active in the dissociation and that the "first" methyl and the "second" methyl are unlikely to have greatly different internal energy distributions.

V. CONCLUSIONS

Time-resolved diode laser absorption/gain spectroscopy has been applied to the 193 nm photodissociation of ace-

tone-d_6 with the following results:

(a) Nascent populations of CD_3 can be characterized by rotational temperatures of 600–750 K in $v_2 = 2,1$, and 0 and a vibrational temperature of 750 K for the ν_2 mode, in reasonable agreement with REMPI measurements of CH_3 fragments from acetone-h_6.[13]

(b) Growth is observed in the vibrationless state on a time scale consistent with vibrational relaxation. The maximum population observed calibrates the total CD_3 yield, and the initial population of the $v = 0$ state is only about $6\% \pm 3\%$ of the total CD_3.

(c) The vibrational state $v_3 = 1$ is not inverted with respect to $v = 0$, based on the positive sign of nascent absorption intensities of several rotational lines in the ν_3 fundamental band. Thus the $v_3 = 1$ state is not the dominant source of growth observed in $v = 0$.

(d) We conclude that the nascent vibrational distribution of CD_3 must be broadly distributed over many accessible states, in a distribution that has as little population in the low vibrational levels as the prior distribution for this dissociation. This is in disagreement with the total vibrational distribution of CH_3 derived from a REMPI study.[13] We ascribe this difference to a low sensitivity of REMPI to vibrationally excited CH_3 due to predissociation, poor Franck–Condon factors, and low populations per quantum state in a broad distribution.

(e) A two-step dissociation with an impulsive first step would produce half the methyl radicals with low internal energy. The small amount of vibrationally cold CD_3 seems inconsistent with this model.

(f) The information-theoretic analysis of Strauss and Houston[23] has been reassessed for this dissociation. The most likely joint probability distribution for the three particles shows no correlation between the recoil directions of the coincident methyl radicals, as would occur in a fully stepwise dissociation. This change in interpretation from the previous calculation is not due to the changed data for the methyl distribution, but rather due to correcting an overly severe approximation in the earlier calculations.

ACKNOWLEDGMENTS

This work was performed at Brookhaven National Laboratory under Contract No. DE-AC02-76CH00016 with the U. S. Department of Energy and supported by its Division of Chemical Sciences. One of us (D. V. B.) gratefully acknowledges support from the Department of Energy's Division of University and Industry Programs, Office of Energy Research, as a Lab Co-op Program participant. We are grateful to Professor P. L. Houston for discussions and for sharing the programs developed in Refs. 22 and 23.

[1] R. B. Cundall and A. S. Davies, Prog. React. Kinet. **4**, 149 (1967).
[2] E. K. Lee and R. S. Lewis, Adv. Photochem. **12**, 1 (1980).
[3] G. D. Greenblatt, S. Ruhman, and Y. Haas, Chem. Phys. Lett. **112**, 200 (1984).
[4] A. Gandini and P. A. Hackett, J. Am. Chem. Soc. **99**, 6195 (1977).
[5] E. L. Woodbridge, T. R. Fletcher, and S. R. Leone, J. Phys. Chem. **92**, 5387 (1988).
[6] P. Potzinger and G. Von Bünau, Ber. Bunsenges, Phys. Chem. **72**, 1908 (1971).
[7] M. Brouard, M. T. MacPherson, M. J. Pilling, J. M. Tulloch, and A. P. Williamson, Chem. Phys. Lett. **113**, 413 (1985).
[8] P. D. Lightfoot, S. P. Kirwan, and M. J. Pilling, J. Phys. Chem. **92**, 4938 (1988).
[9] M. Baba, H. Shinohara, N. Nishi, and H. Hirota, Chem. Phys. **83**, 221 (1984).
[10] G. A. Gaines, D. J. Donaldson, S. J. Strickler, and V. Vaida, J. Phys. Chem. **92**, 2762 (1988).
[11] D. J. Donaldson, G. A. Gaines, and V. Vaida, J. Phys. Chem. **92**, 2766 (1988).
[12] D. J. Donaldson and S. R. Leone, J. Chem. Phys. **85**, 817 (1986).
[13] K. A. Trentelman, S. H. Kable, D. B. Moss, and P. L. Houston, J. Chem. Phys. **91**, 7498 (1989).
[14] A. M. Halpern and W. R. Ware, J. Chem. Phys. **54**, 1271 (1971).
[15] G. E. Hall, T. J. Sears, and J. M. Frye, J. Chem. Phys. **90**, 6234 (1989).
[16] T. J. Sears G. E. Hall, and J. J. F. McAndrew, J. Chem. Phys. **91**, 5201 (1989).
[17] T. J. Sears, J. M. Frye, V. Spirko, and W. Kraemer, J. Chem. Phys. **90**, 2125 (1989).
[18] D. J. Donaldson and S. R. Leone, J. Phys. Chem. **91**, 3128 (1987).
[19] W. M. Fawzy, T. J. Sears, and P. B. Davies, J. Chem. Phys. **92**, 7021 (1990).
[20] H. E. van den Bergh, Chem. Phys. Lett. **43**, 201 (1976).
[21] J. J. Sloan and E. J. Kruus, Adv. Spectrosc. **18**, 219 (1989).
[22] C. E. M. Strauss, Ph. D. thesis, Cornell University, Ithaca, 1990.
[23] C. E. M. Strauss and P. L. Houston, J. Phys. Chem. **94**, 8751 (1990).
[24] We are grateful to Prof. Houston for his assistance in these calculations.
[25] G. E. Hall and P. L. Houston (in preparation).